

Raman modes of $R\text{Ni}_2\text{B}_2\text{C}$ ($R=\text{Lu}, \text{Ho}, \text{Y}$) single crystals

Hyun-Jung Park, Hye-Soo Shin, Hye-Gyong Lee, and In-Sang Yang*
Department of Physics, Ewha Womans University, Seoul, 120-750, Korea

W. C. Lee
Department of Physics, Sookmyung Women's University, Seoul, 140-742, Korea

B. K. Cho, P. C. Canfield, and D. C. Johnston
Ames Laboratory and Department of Physics and Astronomy, Iowa State University, Ames, Iowa 50011
 (Received 14 July 1995)

Results of Raman measurements on $R\text{Ni}_2\text{B}_2\text{C}$ ($R=\text{Lu}, \text{Ho}, \text{Y}$) single crystals are reported. Raman peaks are observed at 190 cm^{-1} and near 830 cm^{-1} . From the polarization-dependence measurements, these peaks are assigned to be the Ni-B_{1g} and the B-A_{1g} modes, respectively. Raman study on the effects of boron isotope ^{10}B substitution for ^{11}B in the $\text{LuNi}_2\text{B}_2\text{C}$ crystals confirms that the mode near 830 cm^{-1} is due to the vibration of B atoms. However, from these single crystals, the expected Ni-E_g and B-E_g modes are not observed.

I. INTRODUCTION

Recently, superconductivity in the Ni-containing alloy systems $R\text{-Ni-B-C}$ ($R=\text{rare earth element}$) was discovered, and soon the $\text{YNi}_2\text{B}_2\text{C}$ phase was identified to be responsible for the superconductivity.^{1,2} For $R=\text{Lu}, \text{Ho},$ and Y , the superconducting transition temperatures (T_c) are found to be $\approx 16, 8,$ and 15 K , respectively. These borocarbides show, however, antiferromagnetic (AF) ordering with its ordering Néel temperatures (T_N) comparable to superconducting T_c . Due to the wide range of T_N , together with relatively high values of T_c , there are good possibilities of observing the interplay between magnetism and superconductivity in these systems.³

These superconductors are considered to be similar to conventional superconductors, where strong electron-phonon scattering is responsible for the pairing mechanism.⁴ Raman spectroscopy is a good probe in investigating the phonon modes as well as the electronic scattering relevant to the phonon-electron interaction in the superconductors. However, there is no conclusive report on Raman modes of single crystals of these systems, except for a couple of articles on polycrystalline $\text{YNi}_2\text{B}_2\text{C}$ samples.^{5,6}

In this paper, results of Raman mode assignments on the $R\text{Ni}_2\text{B}_2\text{C}$ ($R=\text{Lu}, \text{Ho}, \text{Y}$) single crystals are reported. The Raman active modes are observed at 190 cm^{-1} and near 830 cm^{-1} . From the polarization-dependence measurements, these modes are assigned to be the Ni-B_{1g} and the B-A_{1g} modes, respectively. By the study of boron isotope ^{10}B substitution for ^{11}B in the $\text{LuNi}_2\text{B}_2\text{C}$ crystals, it is confirmed that the mode near 830 cm^{-1} is originated from the vibration of B atoms. From the $R\text{Ni}_2\text{B}_2\text{C}$ ($R=\text{Lu}, \text{Ho}, \text{Y}$) single crystals, E_g modes of Ni and B atoms were not observed, contrary to the previous reports on polycrystalline $\text{YNi}_2\text{B}_2\text{C}$ samples.

II. EXPERIMENT

High purity single crystals of $R\text{Ni}_2\text{B}_2\text{C}$ ($R = \text{Lu}, \text{Ho}, \text{Y}$) were grown by the high-temperature flux method, described

elsewhere.⁷ The crystals are thoroughly examined by powder x-ray diffraction, magnetization,⁸ specific heat,⁹ and neutron scattering measurements.³ The powder x-ray-diffraction pattern of pulverized single crystals contains all the peaks matched to those of the $R\text{Ni}_2\text{B}_2\text{C}$ phase with no trace of the second phase. Sometimes only the most intensive line (211) of Ni_2B is observed and is due to a small amount of the flux remaining on the surface of the crystals.

Raman measurements were done at room temperature using a Jobin Yvon U1000 double monochromator in a back-scattering geometry. The spectra were excited with either the 488.0 or 514.5 nm line of an Ar-ion laser focused on surfaces of the crystals through an Olympus metallurgical microscope. The incident laser beam was linearly polarized, and the polarization of the scattered light was analyzed in either parallel or perpendicular direction to the polarization of the incident beam. The spectrometer slit widths were set at $500\text{ }\mu\text{m}$, which corresponds to a resolution of 4 cm^{-1} over the spectral range of interest. Care was taken not to heat the crystals with the excessive power of the laser beam. The beam power of less than 0.1 mW was delivered to an area of $\approx 30\text{ }\mu\text{m}^2$ using $\times 50$ objective lenses.

III. RESULTS AND DISCUSSION

Figure 1 shows the Raman spectra of the $\text{LuNi}_2\text{B}_2\text{C}$ ($^{10}\text{B}, ^{11}\text{B}$), $\text{HoNi}_2\text{B}_2\text{C}$, $\text{YNi}_2\text{B}_2\text{C}$ single crystals and the Ni_2B flux polycrystals. The spectra are excited by either the 514.5 nm line [1(a)] or the 488.0 nm line [1(b)] of the Ar-ion laser, for the following reason. The Raman spectra obtained using the 514.5 nm line have fluorescent peaks of the objective lenses at near $840, 910,$ and 925 cm^{-1} , interfering with the Raman mode at near 830 cm^{-1} . On the other hand, the spectra excited by the 488.0 nm line show plasma lines at $104, 222,$ and 351 cm^{-1} obscuring peaklike features nearby. However, there is no difference between the intrinsic Raman spectra excited by the 514.5 nm line and those excited by the 488.0 nm line.

There are common peaks at near 190 and 830 cm^{-1} for

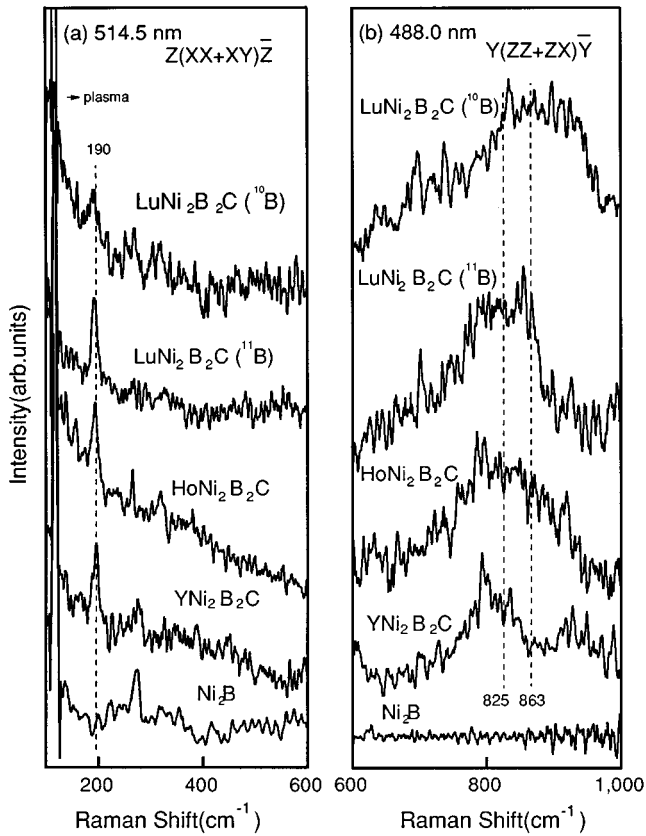


FIG. 1. Raman spectra of $R\text{Ni}_2\text{B}_2\text{C}$ ($R = \text{Lu, Ho, Y}$) single crystals and Ni_2B flux polycrystals. The spectra were excited by the 514.5 nm line (a) and the 488.0 nm line (b) of an Ar-ion laser, for the reason given in the text. The spectra of $R\text{Ni}_2\text{B}_2\text{C}$ in (a) are from the $Z(\overline{XX+XY})\overline{Z}$ geometry and in (b) are from the $Y(\overline{ZZ+ZX})\overline{Y}$ geometry.

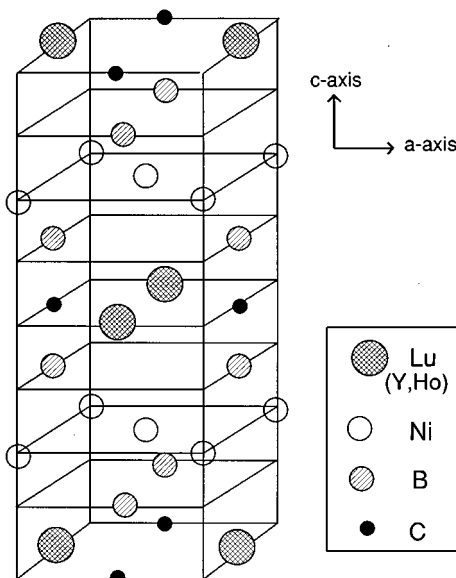


FIG. 2. A schematic drawing of the crystal structure of $R\text{Ni}_2\text{B}_2\text{C}$.

TABLE I. The atoms in $R\text{Ni}_2\text{B}_2\text{C}$ ($R = \text{Lu, Ho, Y}$) crystals are listed along with the Wyckoff notation in the tetragonal body-centered space group $I4/mmm - D_{4h}^{17}$. The irreducible representations of the corresponding point groups are given for all the occupied sites. The sum of the normal modes is given below according to the spectral activity.

Atom	Wyckoff notation	Irreducible representation
R (Lu, Ho, Y)	$2a$	$A_{2u} + E_u$
C	$2b$	$A_{2u} + E_u$
Ni	$4d$	$B_{1g} + E_g + A_{2u} + E_u$
B	$4e$	$A_{1g} + E_g + A_{2u} + E_u$
Acoustic mode		$A_{2u} + E_u$
IR active mode		$3A_{2u} + 3E_u$
Raman active mode		$A_{1g} + B_{1g} + 2E_g$

all the borocarbide single crystals measured in this study. No other Raman modes beyond the noise level are observed from these borocarbide crystals. On the other hand, the Ni_2B flux polycrystals have only one peak near 280 cm^{-1} . The peaks at 118 cm^{-1} in the spectra of Fig. 1(a) are due to the plasma line close to the 514.5 nm line of the Ar-ion laser, and serve as the marker in calibrating the Raman frequency.

Factor group analysis is used in assigning the modes shown in Fig. 1. The Ni_2B crystal belongs to the tetragonal space group $I4/mcm (D_{4h}^{18})$.¹⁰ The Raman active modes of Ni_2B are the A_{1g} , B_{1g} , and E_g modes of Ni atoms at Wyckoff site ($8h$). The vibrations of B atoms in the Ni_2B crystal are not active in Raman. Therefore, the mode near 280 cm^{-1} is believed to be from Ni atoms in the Ni_2B crystal.

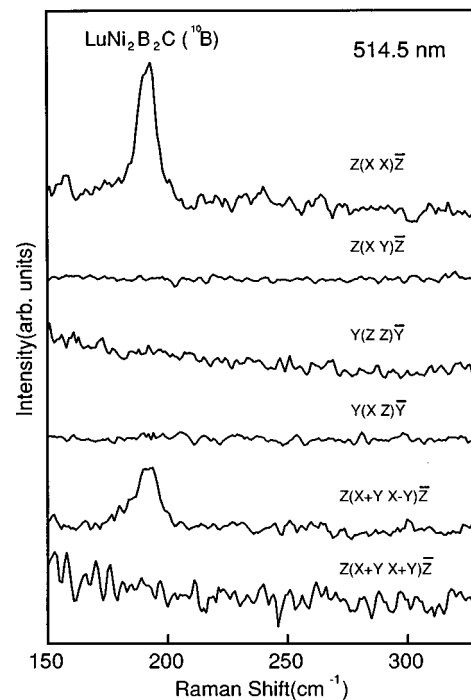


FIG. 3. Raman spectra of the $\text{LuNi}_2\text{B}_2\text{C}$ (^{10}B) single crystal in the range of $150\text{--}330 \text{ cm}^{-1}$ in different geometries. The mode near 190 cm^{-1} shows the B_{1g} symmetry. Note that no additional mode is observed in this spectral range.

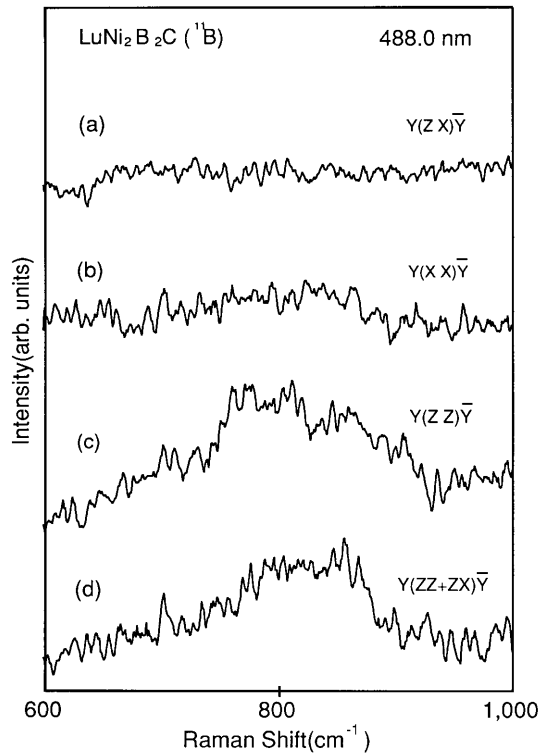


FIG. 4. Raman spectra of the $\text{LuNi}_2\text{B}_2\text{C}$ (^{11}B) single crystal in the range of $600\text{--}1000\text{ cm}^{-1}$ in several geometries. The broad mode near 830 cm^{-1} shows the A_{1g} symmetry.

The symmetry of the mode needs to be found by studying Raman spectra of the Ni_2B single crystals.

The crystal structure of the $\text{RNi}_2\text{B}_2\text{C}$ borocarbides (Fig. 2) is the tetragonal body-centered space group $I4/mmm(D_{4h}^{17})$.^{2,10} Table I summarizes the atomic sites and the possible vibrational modes of these systems. The analysis shows that the Raman active modes of the $\text{RNi}_2\text{B}_2\text{C}$ crystals are the $B_{1g} + E_g$ modes of Ni atoms and the $A_{1g} + E_g$ modes of B atoms.

In general, the intensity of the E_g modes is weaker than that of A_{1g} or B_{1g} modes. Therefore, the two peaks appearing in Fig. 1 are believed to be the B_{1g} mode of Ni atoms and the A_{1g} mode of B atoms. It is natural that the vibrational frequency of the heavier atom Ni is lower than that of the lighter atom B. Thus the mode at 190 cm^{-1} is identified to be from the Ni- B_{1g} mode, and that near 830 cm^{-1} , the B- A_{1g} mode.

Since the mode near 830 cm^{-1} is due to B atoms, it is expected that the frequency of this mode be shifted in the ratio of the square root of the mass ratio of ^{11}B and ^{10}B . As shown in Fig. 1, the Raman frequency obtained from Lorentzian fitting of the B mode of $\text{LuNi}_2\text{B}_2\text{C}$ (^{10}B) is close to 863 cm^{-1} , which is about 40 cm^{-1} higher than that (near 825 cm^{-1}) of $\text{LuNi}_2\text{B}_2\text{C}$ (^{11}B). However, the full width at half maximum (FWHM) values of the boron peaks are about 100 cm^{-1} , i.e., the B modes are extremely broad that the exact values of the Raman frequencies are not meaningful. The broadness may have some relation with the interaction between this phonon mode and other electronic excitations.

The frequency of the boron mode is relatively high, reflecting the strong B-Ni and B-C bonds.² Theoretical calcu-

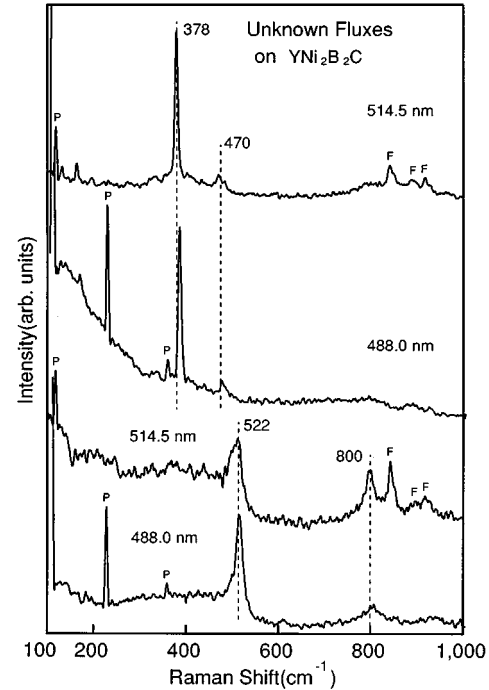


FIG. 5. Some Raman spectra from unknown fluxes remaining on the surfaces of the $\text{YNi}_2\text{B}_2\text{C}$ single crystals. Peaks at 378 , 470 , 522 , and 800 cm^{-1} are observed. The peaks denoted by P are from the plasma lines of the Ar-ion laser. The peaks denoted by F are from the fluorescence of the coating material of the objective lenses.

lations suggested that high frequency of the Raman modes might enhance T_c of these borocarbides.¹¹ However, the Raman frequencies of the Ni and B modes of the $\text{RNi}_2\text{B}_2\text{C}$ ($R = \text{Lu, Ho, Y}$) single crystals at room temperature do not depend on the element R , whereas their T_c values do. It is also noted that the Raman spectra of polycrystalline $\text{YNi}_2\text{B}_2\text{C}$ samples at low temperatures measured by Litvinchuk *et al.* show no appreciable change in frequencies of the Raman modes.⁶

The spectra in Fig. 3 are the results of polarization-dependence measurements of the 190 cm^{-1} mode of $\text{LuNi}_2\text{B}_2\text{C}$. The mode near 190 cm^{-1} appears only in $Z(\text{XX})\bar{Z}$ and $Z(\text{X}+\text{Y}, \text{X}-\text{Y})\bar{Z}$ geometry, while not in $Z(\text{XY})\bar{Z}$, $Y(\text{ZZ})\bar{Y}$, $Y(\text{XZ})\bar{Y}$ and $Z(\text{X}+\text{Y}, \text{X}+\text{Y})\bar{Z}$ geometry. These results confirm that the mode near 190 cm^{-1} is the Ni- B_{1g} mode.

TABLE II. Summary of the frequencies of the Raman modes observed in present measurements on $\text{RNi}_2\text{B}_2\text{C}$ ($R = \text{Lu, Ho, Y}$) single crystals. For comparison, the last column shows the previous results on polycrystalline $\text{YNi}_2\text{B}_2\text{C}$ samples (Ref. 5).

Modes	Lu(^{10}B) ^a	Lu(^{11}B) ^a	Ho ^a	Y ^a	Y(poly) ^b
Ni- B_{1g}	190	191	194	193	198
Ni- E_g					282
B- E_g					470
B- A_{1g}	863	825	829	823	832

^aPresent work.

^bBy Hadjiev *et al.*

The polarization-dependent spectra for the other mode near 830 cm^{-1} is shown in Fig. 4. This mode appears in $Y(ZZ)\bar{Y}$ and very weakly in $Y(XX)\bar{Y}$ but not in $Y(ZX)\bar{Y}$ geometry, which is consistent with the A_{1g} symmetry of the mode. The XX or YY component of the scattering tensor for this mode appears to be much smaller than the ZZ component, thereby the peak intensity in $Y(XX)\bar{Y}$ geometry is weaker than that in $Y(ZZ)\bar{Y}$ geometry.

Contrary to the report by Hadjiev *et al.*,⁵ the $\text{Ni-}E_g$ and $\text{B-}E_g$ modes were not observed from the $\text{RNi}_2\text{B}_2\text{C}$ single crystals. From polycrystalline $\text{YNi}_2\text{B}_2\text{C}$ samples, Hadjiev *et al.* reported four Raman-active modes at 198 cm^{-1} ($\text{Ni-}B_{1g}$), 282 cm^{-1} ($\text{Ni-}E_g$), 470 cm^{-1} ($\text{B-}E_g$), and 832 cm^{-1} ($\text{B-}A_{1g}$). We observe a Raman peak at 280 cm^{-1} from the Ni_2B flux crystals (Fig. 1). In addition, some unknown fluxes remaining on the surface of the $\text{YNi}_2\text{B}_2\text{C}$ single crystals were found to show several peaks at 378 , 470 , 522 , and 800 cm^{-1} (see Fig. 5). Therefore, the modes reported previously at 282 and 470 cm^{-1} are conjectured to be from the intergrain material in the polycrystalline $\text{YNi}_2\text{B}_2\text{C}$ samples. The results of our current work are summarized in Table II, along with those from the previous measurements on polycrystalline $\text{YNi}_2\text{B}_2\text{C}$ samples.

In summary, Raman modes of $\text{RNi}_2\text{B}_2\text{C}$ ($R = \text{Lu, Y, Ho}$) single crystals were studied. All the single crystals show two peaks; one at 190 cm^{-1} and the other at near 830 cm^{-1} . The mode at 190 cm^{-1} is assigned to be the $\text{Ni-}B_{1g}$ mode and the broad mode near 830 cm^{-1} , the $\text{B-}A_{1g}$ mode, from the polarization-dependence analysis of the Raman spectra. Raman study on the effects of isotope ^{10}B substitution for ^{11}B in the $\text{LuNi}_2\text{B}_2\text{C}$ crystals supports that the mode near 830 cm^{-1} is from the vibration of B atoms. The $\text{Ni-}E_g$ and $\text{B-}E_g$ Raman modes, which were reported previously from $\text{YNi}_2\text{B}_2\text{C}$ polycrystalline samples, were not observed from the $\text{RNi}_2\text{B}_2\text{C}$ single crystals.

ACKNOWLEDGMENTS

I.S.Y. was supported by the Korea Science and Engineering Foundation under Contract No. 95-0702-03-01-3. W.C.L. was supported by the nondirected Research Fund, Korea Research Foundation. Ames Laboratory is operated for the U.S. Department of Energy by Iowa State University under Contract No. W-740-Eng-82 and work there was supported by the Director for Energy Research, Office of Basic Energy Sciences.

*Corresponding author.

¹R.J. Cava, H. Takagi, H.W. Zandbergen, J.J. Krajewski, W.F. Peck, Jr., T. Siegrist, B. Batlogg, R.B. van Dover, R.J. Felder, K. Mizuhashi, J.O. Lee, H. Eisaki, and S. Uchida, *Nature* **367**, 252 (1994).

²T. Siegrist, H.W. Zandbergen, R.J. Cava, J.J. Krajewski, and W.F. Peck, Jr., *Nature* **367**, 254 (1994).

³A.I. Goldman, C. Stassis, P.C. Canfield, J. Zarestky, P. Dervenis, B.K. Cho, D.C. Johnston, and B. Sternlieb, *Phys. Rev. B* **50**, 9668 (1994).

⁴W.E. Pickett and D.J. Singh, *Phys. Rev. Lett.* **72**, 3702 (1994).

⁵V.G. Hadjiev, L.N. Bozukov, and M.G. Baychev, *Phys. Rev. B* **50**,

16 726 (1994).

⁶A.P. Litvinchuk, L. Börjesson, N.X. Phuc, and N.M. Hong, *Phys. Rev. B* **52**, 6208 (1995).

⁷B.K. Cho, P.C. Canfield, L.L. Miller, D.C. Johnston, W.P. Beyermann, and A. Yatskar, *Phys. Rev. B* **52**, 3684 (1995).

⁸M. Xu, P.C. Canfield, J.E. Ostenson, D.K. Finnemore, B.K. Cho, Z.R. Wang, and D.C. Johnston, *Physica C* **227**, 321 (1994).

⁹P.C. Canfield, B.K. Cho, D.C. Johnston, D.K. Finnemore, and M. F. Hundley, *Physica C* **230**, 397 (1994).

¹⁰B.C. Chakoumakos and M. Paranthaman, *Physica C* **227**, 143 (1994).

¹¹L.F. Mattheiss, *Phys. Rev. B* **49**, 13 279 (1994).